

# Unique adsorption behavior of H<sub>2</sub> and CO over group 8–10 metals encapsulated inside silica nanotubes and nanocapsules

Shuichi Naito,\* Masato Ue, Seiko Sakai and Toshihiro Miyao

Received (in Cambridge, UK) 18th November 2004, Accepted 5th January 2005

First published as an Advance Article on the web 26th January 2005

DOI: 10.1039/b417396a

Various silica nanotubes and nanocapsules have been prepared successfully, possessing unique silica walls of selective H<sub>2</sub> permeation and encapsulate group 8–10 metal particles inside and exhibit a marked stabilization effect of H<sub>2</sub> and CO over the metals in the network of silica wall and inside nanoscale cavities.

The synthesis of materials with well-defined nanoscale cavities is currently under intensive investigation because of their potential utility as adsorbents, electron devices and catalysts.<sup>1</sup>

Several years ago Hippe *et al.* reported a novel preparation procedure of Pt-encapsulating silica nanotube by employing fine crystals of Pt ammine complexes as a structure-determining template material.<sup>2,3</sup> However, no investigation has been reported of its adsorption and catalytic properties. We have followed their method<sup>4</sup> by employing [M(NH<sub>3</sub>)<sub>6</sub>]Cl<sub>3</sub> (M = Ru, Rh and Ir) and [Pd(NH<sub>3</sub>)<sub>4</sub>]Cl<sub>2</sub> complexes as structure determining template materials. By hydrolyzing tetraethylorthosilicate (TEOS) selectively around the surface of these crystals, hollow silica nanotubes and capsules were formed after various heat treatments under vacuum. Fig. 1 shows the TEM images of formed nanocomposite materials, whose shapes were determined by the crystal shapes of the template complexes. In the cases of fiber-shaped nanocrystals of Pt and Pd ammine complexes silica nanotubes (nt) were obtained, whose ends were mostly closed with diameters of 30–40 nm (Pt) and 300–500 nm (Pd), lengths of 400–1000 nm (Pt) and 4–7 μm (Pd), and wall thicknesses of several nm (Pt) and several ten nm (Pd). The black spots inside the tube were Pt and Pd nanoparticles (20–30 nm) that were formed by the decomposition of the template complexes during heat treatments. There also exist tiny metal clusters (0.3–0.5 nm) in the network of SiO<sub>2</sub> walls. In the cases of Ru, Rh and Ir ammine complexes, rectangular nanocapsules (nc) were formed whose side-length was a few hundred nanometres and

wall thickness was several nanometres. Again, they have metal nanoparticles inside the cavity and tiny metal clusters in the network of SiO<sub>2</sub> walls.

Fig. 2 summarizes the amount of H<sub>2</sub> and CO adsorption over various nanocomposite materials against various evacuation temperatures, measured by Omnisorp 100 CX (Beckman Coulter). The adsorption was reproducible after H<sub>2</sub> reduction and evacuation at 673 K. In the case of the Pt nanotube, after lower temperature treatment (623 K), the amount of adsorbed CO was comparable with that of H<sub>2</sub>, which indicates that both gases can permeate into the silica wall and adsorbed on the metal clusters in the silica wall as well as nanoparticles inside the nanocavities. On the other hand, completely different behavior was observed after higher temperature pretreatment (773 K), and the amount of CO(a) was less than 1/10 of H(a), indicating that only H<sub>2</sub> can permeate into the silica wall. Detailed investigation of the heat treatment process by DTG experiments revealed that the decomposition of ammine complexes took place at around

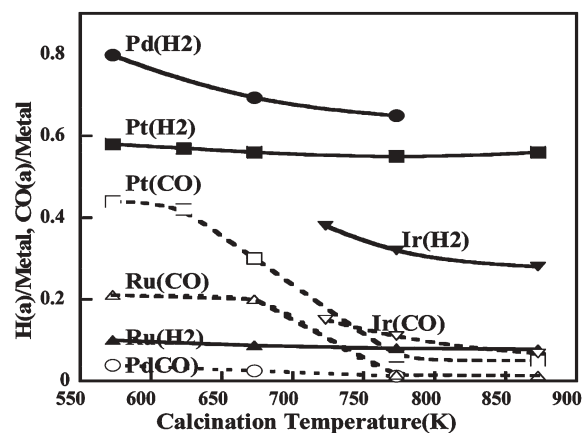


Fig. 2 Dependence of the amount of adsorption upon the calcination temperature.

\*naitos01@kanagawa-u.ac.jp

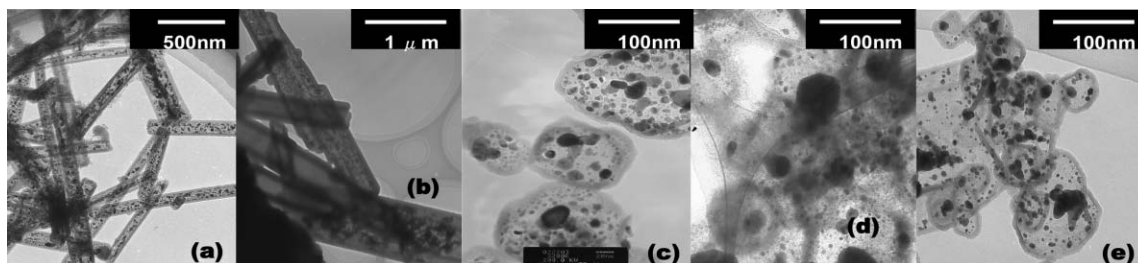


Fig. 1 TEM images of various nanotubes and nanocapsules (a) Pt(nt) (b) Pd(nt) (c) Ru(nc) (d) Rh(nc) (e) Ir(nc).

523–573 K with the evolution of decomposed gases, leaving pores in the silica tube's wall through which both H<sub>2</sub> and CO can permeate. The subsequent high temperature evacuation causes the densification of Si–O–Si bonds and forms ultra-micropores in the silica wall where only H<sub>2</sub> can permeate.

In the case of Pd nanotubes, such a selective permeation of H<sub>2</sub> took place even by 573 K evacuation and the amount of CO(a) was less than 1/50 of H(a). The surprisingly high H(a)/metal ratio of 0.80 suggests the formation of bulk metal hydride, since the Pd particle sizes in the cavity observed by TEM are mostly rather large. Table 1 summarizes the amount of adsorbed H(a) and CO(a) over Pd(nt) and Ru(nc) measured under equilibrium pressure of 150 Torr by a microbalance (Kahn). The H(a)/Pd ratio was 2.1 at 77 K, which is much larger values than the reported bulk hydride (PdH<sub>0.8-0.9</sub>),<sup>5</sup> and suggests the occlusion of H<sub>2</sub> inside the silica nanotubes at lower temperatures.

To investigate the kind of hydrogen adsorbed on Pd(nt), temperature programmed desorption spectra (TPD) were observed over various silica supported Pd catalysts after 150 Torr of H<sub>2</sub> was admitted at 298 K followed by lowering the adsorption temperature to 77 K. Then gaseous H<sub>2</sub> was evacuated at 77 K for 1 h and TPD experiment was started from 77 K. The results were summarized in Fig. 3(a), where vertical axis represents the ratio of the relative amount of H(a) or CO(a) per bulk metal atoms. Generally speaking, desorbed hydrogen from Pd can be divided into two groups: (1)  $\alpha$ -peaks desorbed by the decomposition of subsurface Pd-hydride ( $\alpha_1$  around 160 K and  $\alpha_2$  around 240 K), (2)  $\beta$ -peaks desorbed by the recombination of chemisorbed H(a) from the surface ( $\beta_1$  around 270–350 K and  $\beta_2$  around 370–450 K).<sup>6</sup> In the case of 1 wt.% Pd/SiO<sub>2</sub> catalyst (average particle size of Pd; 2 nm),  $\beta_1$  at 300 K was the main peak together with a small amount of  $\alpha_2$  peak. As the loading amount of Pd was increased to 5 and 10 wt.% (particle sizes; 5–7 nm and 11–13 nm respectively),  $\alpha_2$  became the main peak at 160 K together with a small amount of  $\beta_2$  peak at 370 K. In the case of Pd(nt), the amount of desorbed  $\alpha_2$  hydrogen was twice as much as those of supported catalysts with a shoulder of  $\alpha_1$  peak. The total H/M value estimated from TPD peak was 0.6–0.7, which was similar to that for adsorption at room temperature (0.8) but much lower than that of 77 K adsorption (2.1) under 150 Torr H<sub>2</sub> in Table 1. Accordingly, Pd(nt) can occlude a large amount of H<sub>2</sub> at 77 K, which desorbs quickly by the evacuation at 77 K.

The interesting feature of Ru(nc) is that the amount of adsorbed CO at 298 K was twice as much as that of adsorbed hydrogen over a sample evacuated at lower temperature (<673 K). This situation was even more in the case of 77 K adsorption and three times more CO was adsorbed than H(a). From the TPD result in Fig. 3(b), it is recognized that about half of the adsorbed CO desorbed quickly on evacuation at 77 K. Accordingly, Ru(nc)

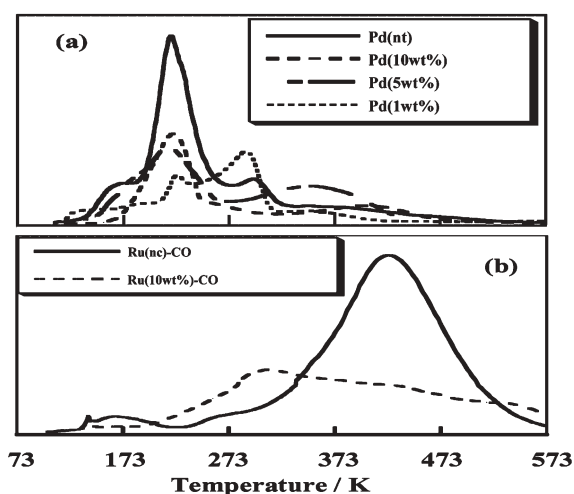


Fig. 3 TPD spectra; (a) H<sub>2</sub> over Pd(nt) and Pd/SiO<sub>2</sub>, and (b) CO over Ru(nc) and Ru/SiO<sub>2</sub>.

seems to occlude a certain amount of CO inside the nanocapsule cavities at 77 K. The TPD peak temperature for adsorbed CO over Ru(nc) (at 430 K) was higher than that over 10 wt.% Ru/SiO<sub>2</sub> catalyst (at 310 K with a long tail up to 570 K), indicating a rather uniform adsorbed state of CO in the case of Ru(nc).

Fig. 4 represents the FT-IR spectra of adsorbed CO over (a) Ru(nc) and (b) 10 wt.% Ru/SiO<sub>2</sub>. In the latter case, a sharp linearly adsorbed CO band was observed at 2054 cm<sup>-1</sup>, which was saturated even under 8 Torr of gaseous CO and desorbed slowly by evacuation at higher temperatures. On the contrary over Ru(nc) under 8 Torr of gaseous CO, a broad band was observed at 2048 cm<sup>-1</sup> which may correspond to the linearly adsorbed CO over 10 wt.% Ru/SiO<sub>2</sub>. By raising gaseous CO pressure, a very sharp band appeared at 2050 cm<sup>-1</sup>, which intensity was almost proportional to the partial pressure of CO up to 100 Torr and disappeared quickly on evacuation at room temperature.

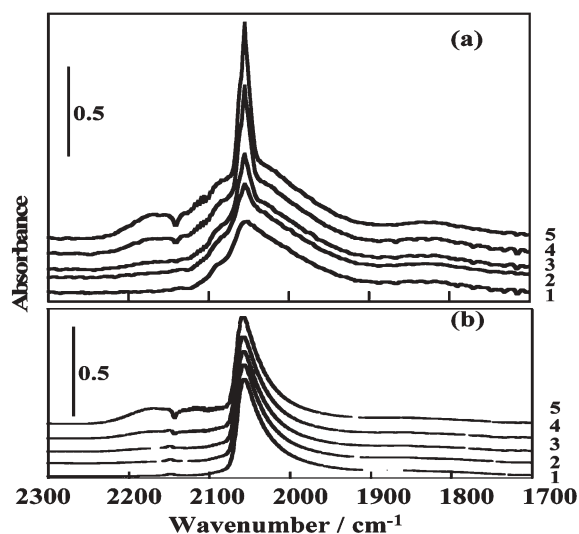


Fig. 4 FT-IR spectra of adsorbed CO over (a) Ru(nc) and Ru(10 wt.%)/SiO<sub>2</sub> 1: 8 Torr, 2: 16 Torr, 3: 27 Torr, 4: 52 Torr, 5: 100 Torr.

Table 1 Amount of H(a) and CO(a) adsorbed ( $P_{\text{eq}} = 150$  Torr)

Metal	Temperature	H/M	CO/M	N <sub>2</sub> /M	Surface area/m <sup>2</sup> g <sup>-1</sup>
Pd(nt) <sup>a</sup>	298 K	0.80	0.04	—	15–20
	77 K	2.1	0.16	0.06	
Ru(nc) <sup>a</sup>	298 K	0.09	0.21	—	100–120
	77 K	0.19	0.62	0.24	

<sup>a</sup> Both samples were evacuated at 573 K.

From these experimental results, it is concluded that the micropores in the silica walls prepared by hydrolyzing TEOS on the surface of ammine complexes containing different metals possess unique gas occlusion character. The pore sizes formed depended on the nature of the structure-determining template ammine complexes, and Pt and Pd nanotubes have smaller micropores inside the silica wall which show preferential for hydrogen occlusion. Ru nanocapsules after lower temperature evacuation seem to have bigger micropores in their silica wall, favorable for CO occlusion. The main adsorption sites for H<sub>2</sub> and CO at room temperature would be metal nanoparticles inside the cavity and tiny metal clusters in the network of SiO<sub>2</sub> walls, which exhibit unique behavior for adsorption. Moreover, physically occluded H<sub>2</sub> and CO may exist in the nanocavities of these metal-oxide nanocomposites at 77 K.

**Shuichi Naito,\* Masato Ue, Seiko Sakai and Toshihiro Miyao**  
*Department of Applied Chemistry, Kanagawa University, 3-27-1, Rokkakubashi, Kanagawa-ku, Yokohama, 221-8686, Japan.*  
*E-mail: naitos01@kanagawa-u.ac.jp; Fax: +81 45 413 9770;*  
*Tel: +81 45 481 5661*

## Notes and references

- 1 G. R. Patzke, F. Krumeich and R. Nesper, *Angew. Chem. Int. Ed.*, 2002, **41**, 2446.
- 2 C. Hippe, M. Wark, E. Lork and G. Schulz-Ekloff, *Microporous Mesoporous Mater.*, 1999, **31**, 235.
- 3 M. Wark, C. Hippe and G. Schulz-Ekloff, *Stud. Surf. Sci. Catal.*, 2000, **129**, 475.
- 4 T. Miyao, T. Saika, Y. Saito and S. Naito, *J. Mater. Sci. Lett.*, 2003, **22**, 543.
- 5 P. C. Aben, *J. Catal.*, 1968, **10**, 224.
- 6 R. J. Behm, V. Penka, M. G. Cattania, K. Christmann and G. Erth, *J. Chem. Phys.*, 1983, **78**, 748.